

Evaluation of the Compression Strength Performance of Fiber-reinforced Polymer (FRP) and Steel-reinforced Laminated Timber Composed of Small-diameter Timber

In-Hwan Lee, Yo-Jin Song, and Soon-Il Hong*

Laminated timber composed of small-diameter timbers reinforced with a steel bar and fiber-reinforced polymer (FRP) were fabricated to satisfy the seismic design performance level of wooden columns, and their compression strength performance was evaluated. The experimental results showed that the average compression strength of the specimen reinforced with a CFRP (Carbon FRP) bar increased by approximately 7% compared to that of the control. The average compression strengths of the specimens reinforced with a GFRP (Glass FRP) bar and a steel bar increased by 38 and 37% compared to that of the control, respectively. The unreinforced control column specimens showed a diagonal failure tendency due to the fiber slope angle, and the wood part of the reinforced specimens showed a failure mode with suppressed diagonal fracture. The average strength of the column reinforced with a CFRP plate increased by approximately 6%, but the average strength of the column reinforced with a GFRP plate decreased by approximately 5%. A comparison of the measured and predicted compression strengths of the specimens showed that the strength differences of all the specimens except the specimen reinforced with a GFRP plate were good (2 to 10.4%).

Keywords: CFRP; Column; Compression strength; FRP; GFRP; Reinforced; FRP-reinforced multi-layer glued column composite

Contact information: Department of Forest Biomaterials Engineering, College of Forest & Environmental Sciences, Kangwon National University, 1, kangwondaehak-gil, ChunCheon-si, Gangwon-do, 24341, Republic of Korea;

* Corresponding author: hongsi@kangwon.ac.kr

INTRODUCTION

Among extreme weather events, earthquakes are almost impossible to forecast, and the damage is mostly concentrated on building structures because the energy is transmitted through the ground. Therefore, seismic design plays a critical role as the only safety measure that can prevent damage from earthquakes. In seismic design, structures must satisfy the functional performance and collapse prevention levels. The functional performance level refers to a structural level where serious structural damage can be prevented and that will allow facilities and structures to maintain their normal functionality after an earthquake. The collapse prevention level, on the other hand, refers to a structural level where large-scale loss of lives and property damage can be prevented while allowing a considerable degree of damage to the structure.

The scope of seismic-design-obligated buildings has expanded recently. In addition, the standards for small-scale building structures are being revised, and methods for the seismic design and reinforcements of steel structures are being implemented (Cozmanciuc *et al.* 2009; Lam *et al.* 2009; Chang *et al.* 2012). The research on the seismic

design and reinforcement of wooden buildings, however, is still insufficient (Attari *et al.* 2019).

Wood has many advantages as a construction material, such as its higher specific strength, elasticity, and shock-absorbing performance compared with other materials. The high specific strength of wood minimizes deformation by inertia during an earthquake, and wooden buildings have a better seismic performance than reinforced-concrete buildings. The column-beam wooden-structure method is the most widely used and oldest wooden building construction method. The column-beam wooden structure is a structure made of columns erected on a foundation and joined by beams as horizontal members. Seismic performance can be secured through appropriate structural forms. Columns are members that form a building space and support the load of the upper part and transmit it to the foundation. When an earthquake occurs, the damage of the column is directly related to the safety of the entire building. Fiber-reinforced polymers (FRPs) with excellent specific strength and durability are appropriate reinforcements for wooden building members and are actively being researched. Small-diameter timber has a low structural performance due to its small cross-sectional area and high juvenile wood content, but it can be used for various types of structural member by increasing the cross-sectional area through multi-layering, and its utilization as a building member is expected.

Larix in Korea takes up 73% of general lumbering industry. Medium-diameter and small-diameter logs produced in the course of thinning takes up the most part of it, or it is produced as logs or chips. Kwon *et al.* (2015) conducted an experimental evaluation of the seismic performance of columns reinforced with FRP seismic reinforcements and reported that the maximum strength and maximum displacement of the reinforced specimen increased by approximately 1.06 to 1.10 and 1.66 to 1.98 times, respectively, compared with the unreinforced specimen. Based on an analytical study on the applicability of fiber-reinforced composites for the improvement of the seismic performance of columns, Jang *et al.* (2012) reported that the carbon-fiber-reinforced polymer (CFRP) plate had higher strength than the glass-fiber-reinforced polymer (GFRP) plate and Hiper Glass. Xiong *et al.* (2016) reinforced timber columns by wrapping them with CFRP for improved strength, but it had a disadvantage of decreasing the aesthetic value. Lee *et al.* (2015) attempted to improve the utilization of a joint in which a GFRP plate was inserted and bonded, reporting that good performance was obtained at the GFP bar thickness and insertion depth of 5 times the diameter. Shin *et al.* (2011) experimented on the compression strength of a multi-layered joint column using domestic small-diameter timber and found that the measured maximum load was proportional to the cross-sectional area.

In this study, columns were fabricated through multi-layer bonding with four small-diameter domestic *Larix* timbers. For the reinforcements, a CFRP plate, a GFRP plate, a CFRP bar, a CFRP bar, and a steel bar were used. Thus, a total of six specimen types were fabricated, including an unreinforced control specimen. Compression strength tests were performed with the fabricated FRP and steel-reinforced glued laminated timber using small-diameter timber, and their strength performances were compared with that of the control. A test specimen was fabricated to increase seismic performance and enhance aesthetic properties. Furthermore, a strength estimation equation was proposed by considering the non-destructive modulus of elasticity of the small-diameter timbers as well as the properties of the reinforcements.

EXPERIMENTAL

Material

For the testing materials, small-diameter domestic *Larix* timbers (60 [T] × 60 [W] × 3600 [L] mm) with a 0.52 average air-dried specific gravity, 16% average water content, and no end-joint were used. The FRP reinforcement uses: a CFRP plate (T: 1.3 mm), a square CFRP bar (6 [T] × 13 [W] mm), a GFRP plate (T: 3.5 mm), and a circular GFRP bar (ϕ : 16 mm) were used. In addition, an SD 350 steel bar (ϕ : 16 mm) was also used as a type of reinforcement (Fig. 1). For wood-wood bonding, PRF (phenol-resorcinol-formaldehyde) adhesive was used. For the bonding of wood with the CFRP plate, GFRP plate, and steel bar, the epoxy (Sikardur-30), polyvinyl acetate (MPU-500), and polyurethane (Ottocoll P84) adhesives were used (Plevris and Triantafillou 1992; Lee *et al.* 2019). The mechanical strength characteristics of all the FRP testing materials were examined through compression and bending strength tests, and the steel bar complied with the strength characteristics of SD 350.

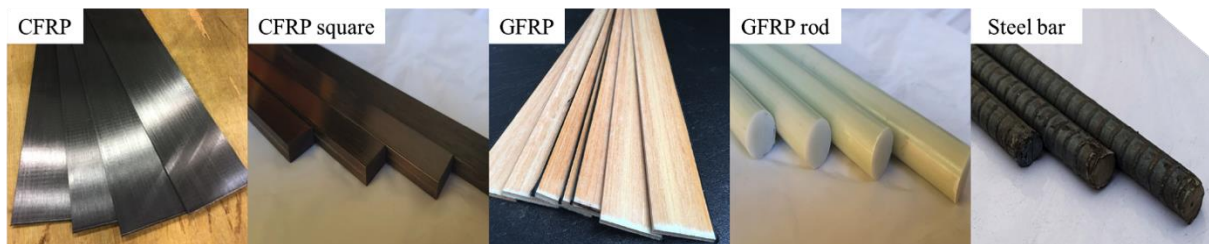


Fig. 1. Photographs of the reinforcements used in this study

Methods

Column specimen fabrication and test methods

To improve the bonding performances of the small-diameter timbers that were used for the columns, those whose adjacent faces were tangential were selected. The slenderness ratio of the specimen was set to 13, and the length was determined to be 450 mm. All specimens were fabricated as 120 × 120 × 450 mm columns with two additional bonds after bonding the reinforcements onto a single small-diameter timber. For the first bonding of the control specimen, 300 g/m² PRF adhesive was applied to two small-diameter timbers, and they were hardened for 24 h at room temperature under 1.5 MPa pressure. The second-bonding surfaces of the first-bonded specimens were sanded, and the second bonding was performed under the same conditions as in the first bonding. The reinforced specimens were joined with the reinforcements before the first bonding, as follows (Fig. 2). The specimen bonded with a CFRP plate was hardened for 24 h at room temperature under 1.5 MPa pressure after being bonded with a single small-diameter timber using 600 g/m² epoxy adhesive. The specimen bonded with a GFRP plate was hardened for 24 h at room temperature after bonding with a single small-diameter timber using 600 g/m² polyvinyl acetate adhesive. The specimen reinforced with a CFRP bar was fabricated under the same bonding conditions as the CFRP plate after pre-processing one surface of a single small-diameter timber (7 × 15 mm) so that the bonding layer would be 1 mm thick. The specimens reinforced with a GFRP bar and a steel bar were bonded by machining 18×18mm square grooves on a single small-diameter timber and then filling them with an adhesive so that the bonding layer thickness between the reinforcement and the timber would be at least 1 mm. Polyvinyl acetate adhesive was used in the small-diameter timber reinforced with a

GFRP bar, and the steel bar and timber were bonded using polyurethane adhesive. The adhesive coating amount and pressure were 300 g/m² and 1.5 MPa, respectively.

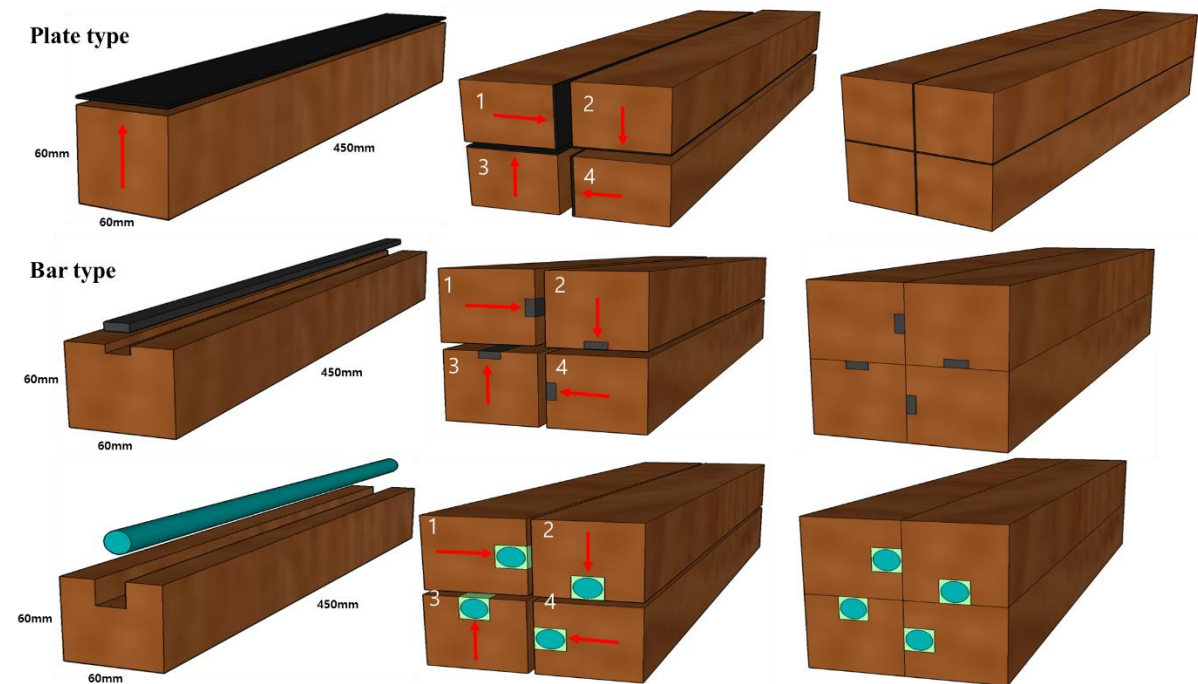


Fig. 2. Shape of the compression strength specimen

Compression strength test

The structural timber compression test was performed by setting the loading rate at 1.35 mm per minute, in accordance with EN 408 (1995). For the compression strength test, a UTM with a maximum load of 200 tons was used, and the displacement and strength were measured simultaneously. The longitudinal compression strength of each specimen was determined by the maximum load and the lateral cross-sectional area of the member. The longitudinal compression modulus of elasticity was determined by the graph slope of the elastic area in the stress-strain graph. The compressive stress and the MOE were calculated by the following formula (Shin *et al.* 2011; Shin *et al.* 2011),

$$\sigma = P_{max}/A$$

$$MOE = P_p L / A \Delta_p$$

where σ is the compressive stress (MPa), MOE is the modulus of elasticity (MPa), P_{max} is the maximum load (N), A is the cross-section of the specimen (mm²), P_p is the proportional limit (mm), L is the length of a specimen (mm), and Δ_p is the proportional limit deformation (mm).

RESULTS AND DISCUSSION

Compressive Strengths of the FRP Reinforcements

The mechanical strengths of the FRP specimens that were used in this study were directly measured. The compression strength test of FRP reinforcements showed that the average compression strength and coefficient of variation of CFRP were 375.7 MPa and

8.62, respectively. The average compression strength of the GFRP bar reinforcements was 160.6 MPa, and the coefficient of variation was 7.65. The measured compression strength of CFRP bar was 234% higher than that of GFRP bar. However, the yield strength of the CFRP bar without considering the cross-sectional area was 26.4 kN, 15% lower than the yield load of the GFRP bar of 30.4 kN. The CFRP specimens all failed in the vertical fiber direction compression strength test. The failure mode of the GFRP compression strength test specimen was fracture of the cross-section. Plate specimens were applied by calculating the experimental results of bar specimens as volume ratio.

Compression Strengths and Moduli of Elasticity of the Column Specimen

The load-deformation curve of the column specimens (Fig. 3) tended to increase gradually from the beginning of loading, and sharply increased from 10 to 20 mm deformation. The column specimens tended to maintain their strength even after failure. The load-deformation curve of the column reinforced with a CFRP plate (Fig. 3) increased gently from the beginning of loading until 14 mm, and then it sharply increased until the failure of the column. The load-deformation curve of the column reinforced with a GFRP plate (Fig. 3) gradually increased from the beginning of loading until 10 mm, and then it sharply increased until failure for three specimens, except GFRP plate-1 and GFRP plate-2. The curve for GFRP plate-1 increased sharply from 19 mm, and that for GFRP plate-2 increased sharply from 15 mm. The average compressive stresses of the column specimens reinforced with a GFRP bar and a steel bar were 59.6 and 59.2 MPa, respectively, which increased by 38 and 37% relative to the 43.3 MPa average compressive stress of the unreinforced control specimen. The average modulus of elasticity also was improved by 5.2 and 21%, respectively. In particular, the specimen reinforced with a steel bar showed a coefficient of variation of 0.88 for stress and a coefficient of variation of 8.79 for modulus of elasticity. Thus, its strength variations depending on the presence or absence of knots were small. The average compressive stress and average compressive modulus of elasticity of the GFRP plate, CFRP plate, and CFRP bar specimens were not significantly different from those of the control specimen.

Table 1. Result of Compression Strength Test

Specimens	P_{\max} Mean (kN)	Reinforcement Volume Ratio	Stress Mean (MPa)	COV (%)	Strain Mean	MOE (MPa)	COV (%)
Control	623.3	0	43.3	4.63	0.063	702	14.48
GFRP plate	590.8	6.19	41.0	7.5	0.06	685.9	11.07
GFRP bar	857.7	5.92	59.6	4.74	0.081	738.8	12.77
CFRP plate	658.8	2.21	45.8	15.12	0.068	671.9	15.68
CFRP bar	665.8	2.21	46.2	7.27	0.072	650.6	12.56
Steel bar	853.0	5.92	59.2	0.88	0.07	853.9	8.79

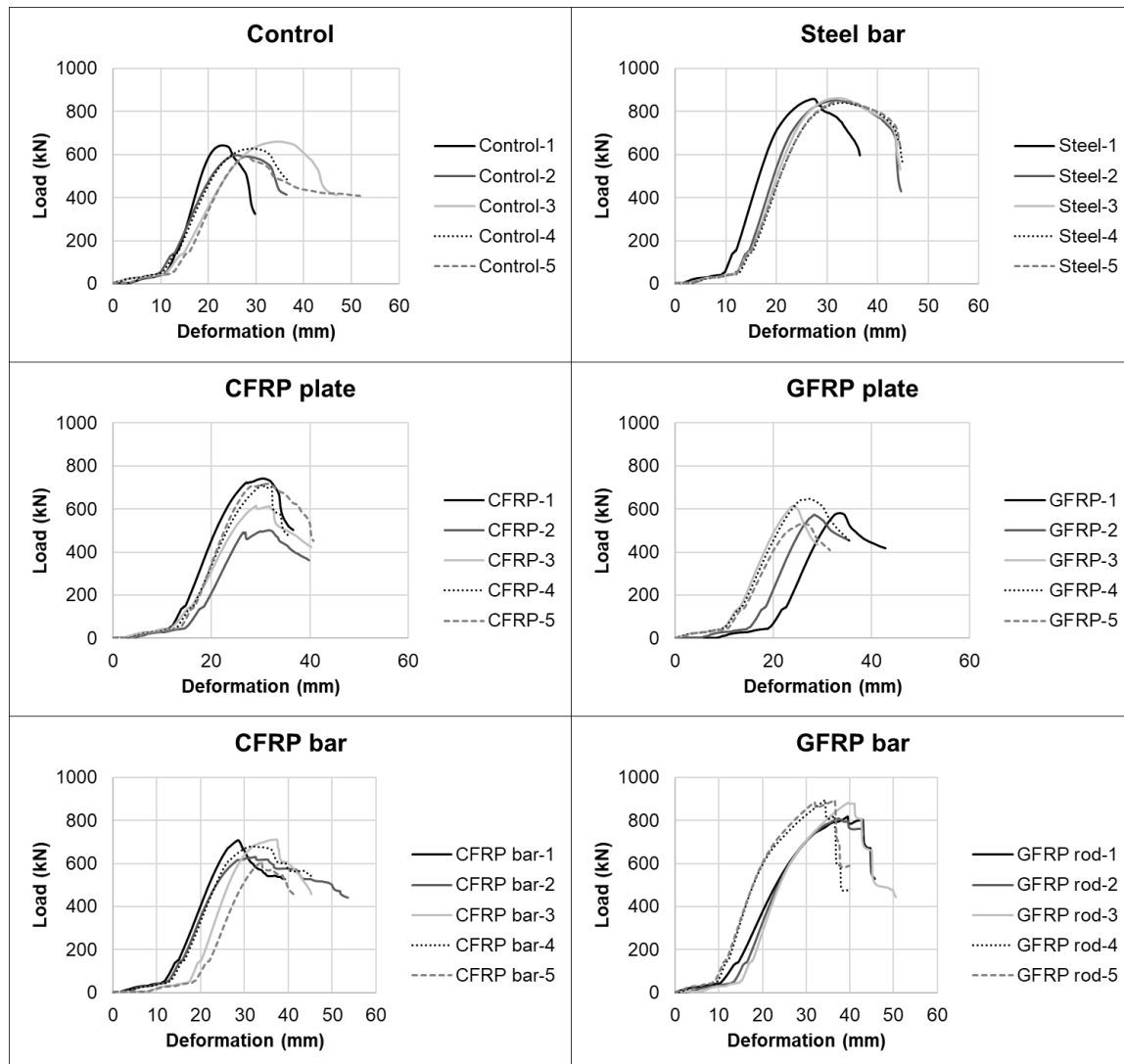


Fig. 3. Load-deformation relationships of the reinforced specimens

Compression Failure Mode of the Column Specimens

The control column specimens showed a diagonal failure tendency due to the fiber slope angle, whereas the wooden part of the reinforced specimens showed a failure mode with suppressed diagonal fracture. The Control-1 specimen showed considerably low strength due to the splitting of the grains parallel to the bond surface. The Control-2 specimen showed lower maximum compression strength than the other specimens due to the failures at four knots. The Control-3 specimen showed high strength due to the few wood defects. The Control-4 specimen showed splitting of the bonded part. For the Control-5 specimen, fractures occurred in the vertical and horizontal directions around the large knots. The control specimen did not show any failure of the bonded layer. CFRP plate-1 showed splitting at the plate-wood bonding part. CFRP plate-2 had no splitting at the plate-wood bonded surface, but showed relatively low strength due to the large failure from the column top to the knot. CFRP plate-3 had no obvious split in appearance but failed because the entire upper part of the column collapsed. CFRP plate-4 had plate-bonded part splitting and CFRP plate failure. In CFRP plate-5, diagonal failure from the top bonded part to the outside occurred. In GFRP plate-1, failure occurred from a large knot in the

middle of the column. In GFRP plate-2, cohesive failure of the GFRP plate was caused by the load. The failure of GFRP plate-3 started by the splitting of the bonded part. In GFRP plate-4, splitting by a knot, splitting of the bonded part, and cohesive failure of the GFRP plate occurred. GFRP plate-5 had a large knot, but no splitting occurred, only cohesive failure of the GFRP plate. GFRP plate is made of phenolic adhesive and is thought to have weak self-intensity.

For all specimens reinforced with a CFRP bar except CFRP bar-3, failure occurred at the top, which was directly under the compressive load. In CFRP bar-3, a fracture occurred from the large knot at the middle-bottom part. Table 1 shows the results of the specimens in which a GFRP bar was inserted and the inside was filled with PVAc, and Fig. 4 shows the failure mode. In all the specimens except GFRP bar-2, the failure started from a knot, and the splitting progressed along the fiber direction. It was observed that the GFRP bars at both cross-sections failed due to compression, as shown in Fig. 4. The GFRP bar-2 specimen was damaged by the occurrence of a brittle fracture of the outer timber from the GFRP bar insertion point, due to the internal stress of the GFRP bar. The wood failed in all the specimens reinforced with steel bars, and the strength variations were small even though failures occurred at large knots.

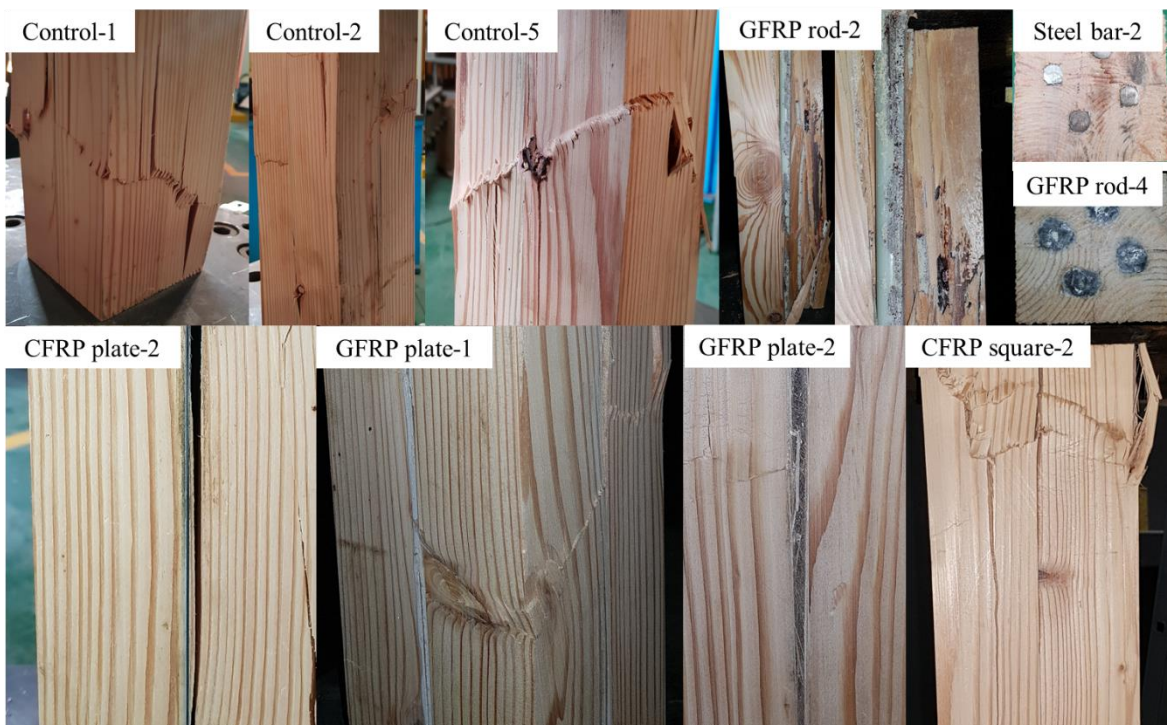


Fig. 4. Photographs of the reinforced-specimen failure modes

Strength Estimation Formula According to the Reinforcement-Volume Ratio of the Column Specimens

The following strength estimation formula of the column specimens (Eq. 1) was used to predict the strength of the composite small-diameter timber by the non-destructive modulus of elasticity of *Larix*. The predicted compression strength was compared with the experimentally determined compression strength (Table 2).

$$F_c = (F_w A_w + F_r A_r) / A \quad (1)$$

In the above equation, F_c is the predicted compression strength (MPa) of the column specimen, F_w is the compression strength of the *Larix* small-diameter timber (MPa), A_w is the wooden area of the cross-section of the column specimen (mm^2), F_r is the compression strength of the reinforcement (MPa), A_r is the reinforcement area of the cross-section of the column specimen (mm^2), and A is the cross-sectional area of the column specimen (mm^2). For the compression strengths of the reinforcements, the following values determined through the preliminary experiment were applied: 285.6 MPa for GFRP, 375.7 MPa for CFRP, and 350 MPa for the SD 350 steel bar.

Table 2. Comparison between Theoretical and Experimental Results

Series	Compressive Strength (MPa)		
	Experimental results	Analytical results	Difference (%)
CON	43.3		
GFRP plate	41.0	50.1	-22
GFRP bar	59.6	49.9	16
CFRP plate	45.8	50.5	-10.2
CFRP bar	46.2	50.5	-9.3
Steel bar	59.2	60.4	-2.0

The comparison of the measured and predicted compression strengths of the column specimens showed that test specimens reinforced with CFRP had a strength deviation of about 10%. For the specimen reinforced with the SD 350 steel bar, the difference between the predicted and measured strengths was small (2%). In contrast, the measured strength of the specimen reinforced with a GFRP plate was 22% lower than the predicted strength. This large difference seems to have been due to the cohesive failure of the GFRP plate. As the performance of not only column timber but also column-beam joint of seismic performance in wooden structure with column-beam structure is considered the most important, various experiments are being done (Jung *et al.* 2016; Lee *et al.* 2017). In the future, seismic performance needs to be reviewed by producing timber, which showed the greatest strength in this study and forms column and joint.

CONCLUSIONS

1. The results of the compression strength test showed that the average strength of the column reinforced with a carbon-fiber-reinforced polymer (CFRP) plate was increased by approximately 6%. In contrast, the average strength of the column reinforced with a glass-fiber-reinforced polymer (GFRP) plate was lower by approximately 5%, which seems to have been due to the cohesive failure of the GFRP plate before the failure through wood defects like knot and cohesive failure.
2. The average strength of the specimen reinforced with a CFRP bar was increased by approximately 7%, while the reinforcement with a GFRP bar increased the average strength by approximately 38%, showing the best reinforcement effect.
3. The strength of the specimen reinforced with a steel bar showed a 37% strength increase compared to the control, and the strength variation depending on the existence or absence of knot was small.
4. When the measured compression strength of the column specimen was compared with

the predicted compression strength, the difference in the strength of the specimen reinforced with a steel bar was found to be only 2%, showing the smallest prediction deviation.

5. All the specimens except the specimen reinforced with a GFRP plate showed good strength variations of 2 to 10.4%. Suppressing fracture due to the fiber slope angle type is considered to have good seismic design performance.
6. It is believed that the reinforced specimens of this study have better aesthetic properties than the wood-steel-wood joints.

ACKNOWLEDGEMENT

This study was conducted as a basic research project supported by Korea Research Foundation with funding from the government (Ministry of Education) in 2016 (No. R1D1A1B01011163)

REFERENCES CITED

- Attari, N., Youcef, Y. S., and Amziane, S. (2019). "Seismic performance of reinforced concrete beam–column joint strengthening by FRP sheets." *Structures* 20, 353-364. DOI: 10.1016/j.istruc.2019.04.007
- Chang, C. H., Kwon, M. H., Kim, J. S., and Joo, C. H. (2012). "Numerical study for seismic strengthening of RC columns using fiber reinforced plastic composite," *Journal of the Korea Institute for Structural Maintenance and Inspection* 16(3). DOI: 10.11112/jksmi.2012.16.3.117
- Cozmanciuc, C., Oltean, R., and Munteanu, V. (2009). "Strengthening techniques of RC columns using fibre reinforced polymeric materials," *Bulletin of the Polytechnic Institute of Jassy, Constructions. Architecture* Section 3(3).
- EN 408 (1995). "Timber structures — Structural timber and glued laminated timber — Determination of some physical and mechanical properties," European Committee for Standardization, Brussels, Belgium.
- Jang, S. J., Song, Y. J., Kang, S. W., Kim, H. R., You, Y. C., and Yun, H. D. (2012). "Shear strength of insulated concrete sandwich wall panels by using different types of insulation," *Korea Concrete Institute*, 5, 387-388.
- Jung, H. J., Song, Y. J., Lee, I. H., and Hong, S. I. (2016). "Lateral load performance evaluation of larch glulam portal frames using GFRP-reinforced laminated plate and GFRP rod," *Journal of the Korean Wood Science and Technology*, 44(1), 30-39. DOI: 10.5658/WOOD.2016.44.1.30
- Kwon, M. H., Seo, H. S., Lim, J. H., Kim, J. S., and Jung, W. Y. (2015). "Experimental seismic performance evaluation on reinforced column with FRP seismic reinforced strip," *The Magazine of the Korean Society for Advanced Composite Structures* 6(2), 25-30.
- Lam, L., and Teng, J. G. (2009). "Stress–strain model for FRP-confined concrete under cyclic axial compression," *Engineering Structures*, 31(2), 308-321. DOI: 10.1016/j.engstruct.2008.08.014
- Lee, I. H., Song, Y. J., and Hong, S. I. (2017). "Evaluation of the lateral strength

- performance of rigid wooden portal frame,” *Journal of the Korean Wood Science and Technology*, 45(5), 535-543. DOI: 10.5658/WOOD.2017.45.1.28
- Lee, I. H., Song, Y. J., Jung, H. J., and Hong, S. I. (2015). “Moment resistance performance evaluation of larch glulam joint bonded in glass fiber reinforced plastic rods,” *Journal of the Korean Wood Science and Technology* 43(1), 60-70. DOI: 10.5658/WOOD.2015.43.1.60
- Plevris, N., and Triantafillou, T. C. (1992). “FRP-reinforced wood as structural material,” *Journal of Materials Civil Engineering* 4(3). DOI: 10.1061/(ASCE)0899-1561(1992)4:3(300)
- Shin, I. J., and Jang, S. S. (2011). “Mechanical property of multi-layer glued timbers manufactured by using bar timbers produced from domestic small diameter logs,” *Graduate School, Chungnam National University*.
- Shin, I. J., Kim, Y. H., and Jang, S. S. (2011). “Compression strength performance of multi-layer glued columns by using square lumbers produced from domestic small diameter logs,” *Korean Journal of Agricultural Science* 38(3), 533-540.
- Xiong, X. Y., Lu, X. X., and Xue, R. J. (2016). “The study on timber pier columns strengthened with Cfrp hoops in ancient architecture,” *Advanced Composites Letters*, 25(6). DOI: 10.1177/096369351602500602

Article submitted: March 3, 2020; Peer review completed: June 13, 2020; Revised version received and accepted: November 2, 2020; Published: November 30, 2020.
DOI: 10.15376/biores.16.1.633-642